Gain Compensated Symmetric Loaded Transmission Line Exhibiting Bidirectional Negative Group Delay

Greg E Bridges[1*], Miodrag Kandic[1]

[1]Electrical and Computer Engineering, University of Manitoba, Winnipeg, Canada
*corresponding author, E-mail: bridges@ee.umanitoba.ca

Abstract

A one-dimensional medium capable of bidirectional lossless negative group delay electromagnetic wave propagation is described. The medium is implemented as a microwave circuit comprising of two symmetric resonator loaded transmission lines, with active gain compensation and coupled through power combiners. We experimentally demonstrate the circuit is conditionally stable and is capable of lossless transmission of a finite bandwidth pulse in both directions. A measured group delay of -600 ps with a gain of 1.12 dB in both directions is achieved for a Gaussian pulse with a bandwidth of 14 MHz modulated at a frequency of 280 MHz (NGD-bandwidth-product of 0.0084). This circuit demonstrates the possibility of constructing a one-dimensional spatial void.

1. Introduction

Media exhibiting superluminal or negative group delay (NGD) have been explored in the optical regime [1] as well as the microwave regime where they are commonly implemented using loaded transmission lines [2]. Passive devices based on resonator loaded transmission lines can provide NGD in regions of anomalous dispersion but are accompanied by loss. Several active circuit designs, which incorporate gain elements, have been proposed to compensate for this loss [3-9]. These circuit topologies are, however, inherently unidirectional. Bidirectional transmission line media have recently been demonstrated that are capable of superluminal group velocity using shunt negative capacitance devices [10], and negative group velocity using symmetric coupled active transmission lines [11]. In this paper we present a bidirectional lossless NGD transmission line and demonstrate measurements of stable time-domain pulse propagation with NGD in both directions through this media.

Circuits exhibiting superluminal or negative group delay have enabled many novel microwave devices through their ability to provide phase equalization or delay compensation. Several passive NGD circuits, mostly based on series or parallel RLC resonators have been reported [2,12,13]. These devices exhibit large attenuation for any reasonable NGD, and there is a trade-off between the achieved NGD and attenuation at the resonance frequency [7]. The attenuation can be compensated by cascading active elements with resonators or by integrating the resonator within the amplifier feedback circuitry. The use of active elements limits the signal transmission in gain-compensated NGD media to be unidirectional and places restrictions on their application. For example, the gain-compensated NGD application in series-fed phased arrays [14,15] can be used for either transmit or receive modes, but not simultaneously. In [11] a symmetric bilateral gain-compensated NGD circuit was presented which enabled a bilateral lossless constant phase shifter. Most studies of NGD microwave devices present the frequency behavior, with few examining the time-domain response to finite bandwidth waveforms and their associated distortion [16].

2. Bidirectional NGD Media

In this paper we present a one-dimensional medium that exhibits NGD without absorption in both directions. The transmission line-based medium enables finite bandwidth transverse electromagnetic pulses to propagate in both directions with NGD and without loss (peak of the output pulse exits the medium before the peak arrives at the input) as shown in Fig. 1.

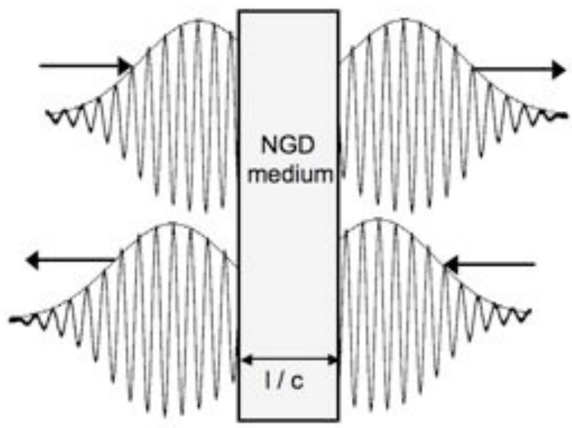

Figure 1: Active bidirectional medium with physical length τ_0=l/c exhibiting lossless negative group delay for finite bandwidth pulses.

The bidirectional NGD medium is implemented using two symmetric resonator-loaded transmission lines with active gain compensation, which are coupled through combiners as shown in Fig. 2. The resonator-loaded transmission lines in each of the branches (A-B) are used to produce the NGD and can be constructed using several different topologies as previously described in [6]. A passive resonator based circuit exhibiting negative group delay will inherently have attenuation associated with it. Attenuation can be compensated by cascading an active gain stage with the NGD circuit. Various approaches, involving cascaded NGD circuit-amplifiers [3], integration of the NGD resonator in the feedback path of an op-amp [7] or use of the out-of-band negative phase characteristic in the roll-off of an amplifier have been used to achieve lossless NGD [17] in transmission line based media. However, all these previous approaches are unidirectional due to the active gain stage in these circuits.

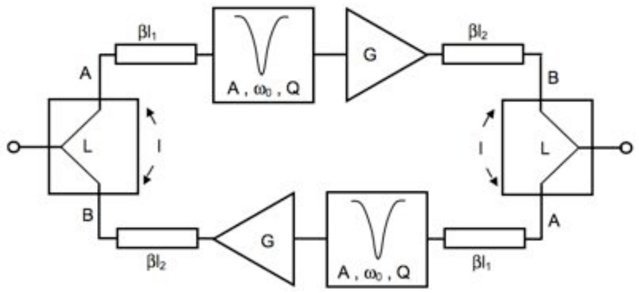

Figure 2: Bidirectional NGD medium implementation using a symmetric coupled resonator-loaded transmission line circuit with active gain compensation.

The 2-port description of the bidirectional circuit in Fig. 2 will be derived by first considering the transmission and reflection coefficients of the individual branches (A-B). Any passive resonator-based NGD circuit comprised of simple matched resonators can be modeled using a cascaded second-order transfer function [7]. For the generic gain-compensated case of Fig. 2, the transmission coefficient of a matched cascaded N-stage resonator design is

$$S_{21}^{AB}(\omega) = G\left[\frac{1 + jQ(\omega/\omega_0 - \omega_0/\omega)}{A_{tot}^{1/N} + jQ(\omega/\omega_0 - \omega_0/\omega)}\right]^N e^{-j\omega\tau_{AB}}, \quad (1)$$

where Q is the chosen quality factor of individual resonators, ω_0 is the resonance frequency, and A_{tot} is the maximum out-of-band magnitude swing of the overall N-stage design ($A_{tot}=A^N$). Here, G is the compensating amplifier gain and compensates for the NGD resonator loss as well as losses in the two combiners such that $|G/A_{tot}|>1$ or $|S_{21}^{AB}(\omega)|>1$. The $exp(-j\omega\tau_{AB}) = exp(-j\beta l_1 - j\beta l_2)$ term accounts for the delay through the finite length transmission lines interconnecting the device components. Expression (1) assumes ideal wideband input and/or output matching of the cascaded stages. The overall N-stage bandwidth is determined by the overall quality factor $Q_{tot}=\omega_0/\Delta\omega$. Assuming $1/(2Q_{tot})<<1$, and with $A_{tot} > 2^{1/2}$ yields [7]

$$Q_{tot} = Q\frac{\sqrt{1-(2/A_{tot}^2)^{1/N}}}{\sqrt{2^{1/N}-1}}. \quad (2)$$

The bidirectional gain-compensated NGD circuit is shown in Fig. 2. It consists of two symmetric gain-compensated NGD branches coupled by two power combiner/splitters with high isolation and low insertion loss. We define the power combiner insertion coefficient, $Lexp(j\phi_L)$, and isolation coefficient, $Iexp(j\phi_I)$. Assuming amplifiers with matched outputs so that $|S_{22}^{AB}(\omega)|=0$, the overall transfer and reflection coefficients for the bidirectional circuit is

$$S_{11} = S_{22} = \left(Le^{j\phi_L}\right)^2 \frac{(S_{21}^{AB})^2 Ie^{j\phi_I} + S_{11}^{AB}}{1-(S_{21}^{AB})^2\left(Ie^{j\phi_I}\right)^2}, \quad (3)$$

$$S_{21} = S_{12} = \left(Le^{j\phi_L}\right)^2 S_{21}^{AB}\frac{1+S_{11}^{AB}Ie^{j\phi_I}}{1-(S_{21}^{AB})^2\left(Ie^{j\phi_I}\right)^2}. \quad (4)$$

At the resonance frequency we note that for combiners with very good isolation, such that $|S_{21}^{AB}I|<<1$ and $|S_{11}^{AB}I|<<1$, the transmission coefficient is $S_{21} = L^2 exp(j2\phi_L)S_{21}^{AB}$.

The transmission coefficient phase and the differential-phase group delay can be expressed, respectively, as

$$\phi(\omega) = \tan^{-1}\left(\frac{\mathrm{Im}(S_{21})}{\mathrm{Re}(S_{21})}\right) \text{ and } \tau_g = -\frac{d\phi(\omega)}{d\omega}. \quad (5)$$

The minimum group delay (largest NGD, if it becomes negative) occurs approximately at the resonance frequency, and can be evaluated from (4) under the ideal combiner isolation assumption, as

$$GD_{21} = \tau_g\Big|_{\omega=\omega_0} = -\frac{2Q_{tot}}{\omega_0}N\sqrt{2^{1/N}-1}\frac{1-1/A_{tot}^{1/N}}{\sqrt{1-(2/A_{tot}^2)^{1/N}}} + \tau_{AB} + 2\tau_L, \quad (6)$$

where τ_{AB} is the positive group delay associated with the physical delay of the NGD circuit (A-B) and τ_L is the group delay due to the coupler and is related to the slope of ϕ_L at the resonant frequency.

2.1. Bidirectional gain-compensated NGD circuit

The constructed bidirectional NGD circuit is shown in Fig. 3a, with its equivalent circuit shown in Fig. 3b. In this work we employ a matched T-network of series/parallel resonators for the NGD passive circuit [13], equivalent to an N=3 stage cascaded second order filter (as modeled by eqn. 1). The resonator is cascaded with a very wideband, low group delay, amplifier with a gain, G_{AMP}, and an attenuator with insertion coefficient L_{ATTN}. The attenuator after the amplifier is used to adjust the total insertion loss of the circuit so that the net gain of the bidirectional circuit is unity ($|S_{21}(\omega_0)|=1$). The shunt capacitor, C_{LP}, acts as a low-pass filter and is incorporated to cause the gain to roll off at high frequencies. When the resonance frequency and quality factor of the cascaded resonators are chosen to be equal, and ignoring C_{LP}, the transmission and reflection coefficients of the individual NGD–gain compensated branches (A-B) is

$$S_{21}^{AB} = G\frac{1}{1+z_p}\frac{2}{2+y_s(1+z_p)}e^{-j\omega\tau_{AB}}, \tag{7}$$

$$S_{11}^{AB} = \frac{1}{1+z_p}\frac{2z_p - y_s(1-z_p^2)}{2+y_s(1+z_p)}e^{-j\omega\tau_{AA}}, \tag{8}$$

where

$$z_p = \frac{R_p/Z_0}{1+jQ\left(\dfrac{\omega}{\omega_0}-\dfrac{\omega_0}{\omega}\right)} \quad , \quad y_s = \frac{Z_0/R_s}{1+jQ\left(\dfrac{\omega}{\omega_0}-\dfrac{\omega_0}{\omega}\right)}, \tag{9}$$

$$Q = Q_p = \frac{R_p}{\sqrt{L_p/C_p}} = Q_s = \frac{\sqrt{L_s/C_s}}{R_s}, \tag{10}$$

$$\omega_0 = \omega_p = \frac{1}{\sqrt{L_pC_p}} = \omega_s = \frac{1}{\sqrt{L_sC_s}}, \tag{11}$$

$$R_s = \frac{Z_0^2 - R_p^2}{2R_p} \quad , \quad A_{tot} = \frac{Z_0+R_p}{Z_0-R_p}. \tag{12}$$

Here $G = G_{AMP}L_{ATTN}$ and is chosen so that $GL^2/A_{tot} = 1$, or $G_{AMP}L_{ATTN} = A_{tot}/L^2$ where L is the insertion coefficient of a single combiner. The resonator lumped element values can be determined from eqns. (10-12) by specifying Q, A_{tot}, f_0 and Z_0. Note that eqn. 12 puts limits on the values of R_p.

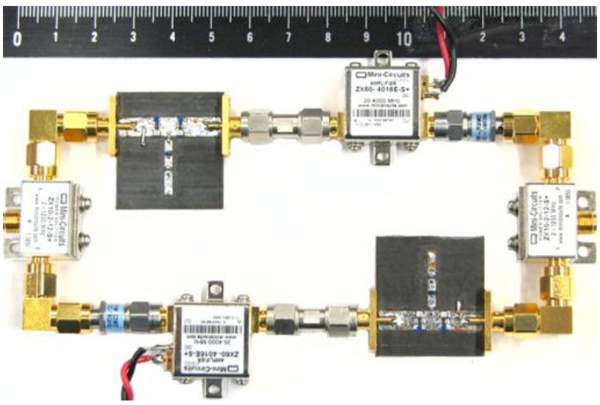

a)

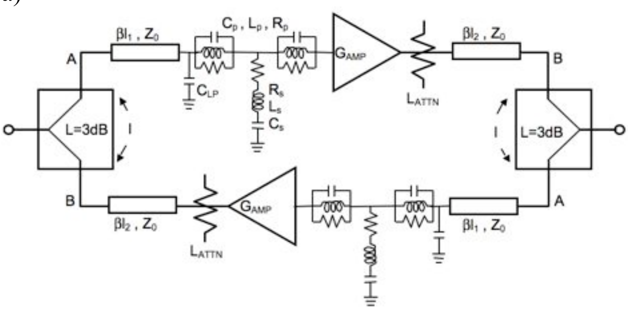

b)

Figure 3a) Bidirectional resonator-loaded transmission line circuit exhibiting lossless NGD and b) its equivalent circuit block diagram.

For our NGD bidirectional medium, a resonant frequency of f_0 = 280 MHz, a Q = 2.62 and an out-of-band gain A_{tot} = 2.84 (9.1 dB) were chosen as design parameters along with a reference impedance $Z_0 = 50\Omega$. For ideal combiners with 3 dB insertion loss ($L=1/2^{1/2}$ and I=0), $G = G_{AMP}L_{ATTN}$ = 5.68 (15.1 dB). The transmission coefficient frequency responses, S_{21}^{AB} as determined using (7) and the N-stage cascaded approximation (1), and S_{21} as determined using (4) for these design parameters is shown in Fig. 4. Using (6) with $\tau_{AB} = \tau_L = 0$, the design provides a theoretical group delay, GD_{21} = -2.63 ns.

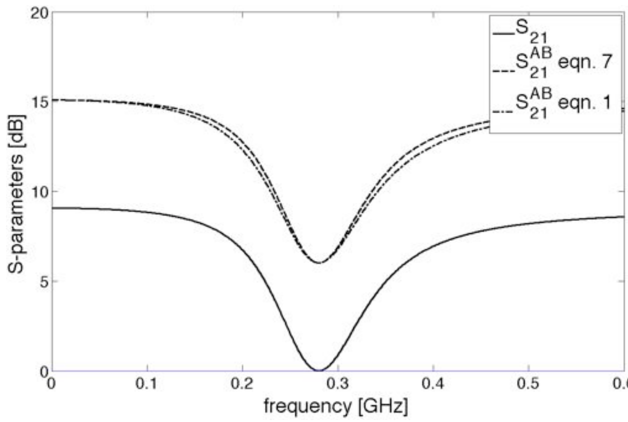

Figure 4: Theoretical transmission coefficients, S_{21}^{AB} and S_{21}, for the design specified by f_0 = 280 MHz, Q = 2.62, A_{tot} = 2.84 and $Z_0 = 50\Omega$, with $L=1/2^{1/2}$ and I=0. The associated GD_{21} = -2.63 ns.

2.2. Measured frequency response and group delay

The bidirectional NGD circuit shown in Fig. 3a was constructed using packaged components interconnected with coaxial transmission line sections (wideband amplifiers, ZX60-4016, power combiners, ZX10-2-12, and attenuators, BW-S3W2, all from Minicircuits). The resonator-based NGD circuit was fabricated using *RT/duroid* 5880 (ε_r = 2.2 and 1.52 mm thickness). The surface mount component values used in the fabricated resonator were $R_p=24\Omega$, L_p=4.7nH, C_p=56pF and $R_s=43\Omega$, L_s=39nH, C_s=6.8pF and C_{LP}=12pF. These differed from the theoretically designed values to compensate for component and printed circuit parasitic effects. The amplifier/attenuator gain, $G_{AMP}L_{ATTN}$ = 17 dB, was designed so the overall gain was slightly over 6 dB at the resonant frequency, in order to compensate for the non-ideal insertion loss of the two combiners. The measured S-parameters of the single-branch gain-compensated NGD circuit (A-B) are shown in Fig. 5a (as measured using an Agilent 8753E Network Analyzer). Also provided are the simulated parameters as calculated using the *Ansoft Designer* circuit simulator. The measured resonance frequency was 280 MHz, with an overall gain at resonance of 7.2 dB. Fig. 5b shows the measured and simulated group delay of the single-branch (A-B) circuit, indicating a measured GD_{21}^{AB} = -1.8 ns. Using measured positive delay values, τ_{AB} = 805 ps and τ_{AA} = 960 ps, eqn. (6) predicts a theoretical group delay GD_{21}^{AB} = -1.82 ns.

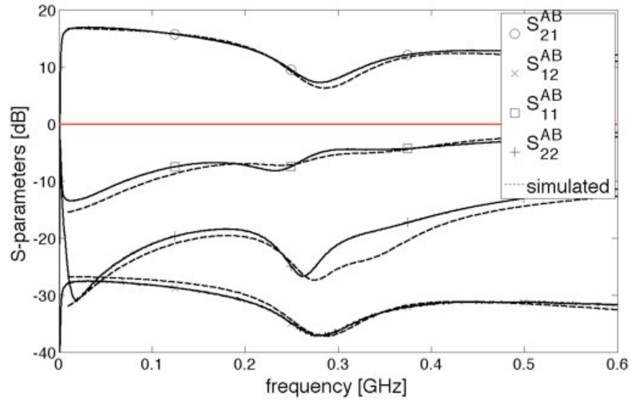

a)

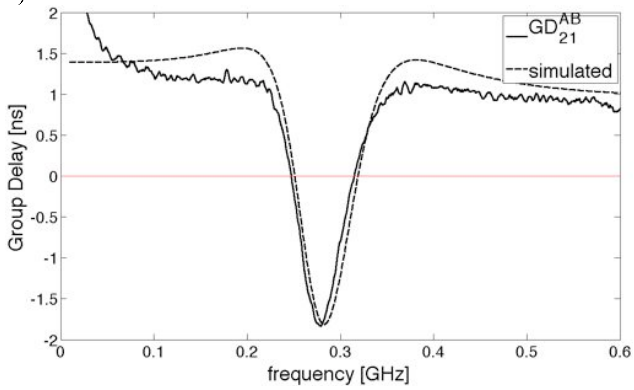

b)

Figure 5a) Measured (solid lines) and simulated (dashed lines) S-parameters of the gain-compensated NGD single branch (A-B) shown in Fig. 3b and b) its measured and simulated group delay.

The measured and simulated *S*-parameters and group delay of the overall bilateral circuit shown in Fig. 3 are given in Fig. 6a and Fig. 6b, respectively. For matched terminations at both ports, the measured circuit is stable at all frequencies (both $|S_{11}|$ and $|S_{22}|$ are below 0 dB). The transmission coefficients in both directions at the resonance frequency are compensated ($|S_{21}|$ and $|S_{12}|$ are both 0.38 dB), providing lossless bidirectional propagation. The circuit exhibits a measured negative group delay, GD_{21} = -0.85 ns at the resonance frequency, in both directions. This includes the delay of the amplifier, the splitter/combiners and the interconnecting transmission lines. Using the measured positive delay of the combiner, τ_L = 332 ps, eqn. (6) predicts a theoretical group delay GD_{21} = -1.16 ns. The speed-of-light delay across the physical length of the circuit (14.5 cm) in air would be 483ps. The negative group delay produced by this circuit would enable compensating for a total physical length of 40 cm.

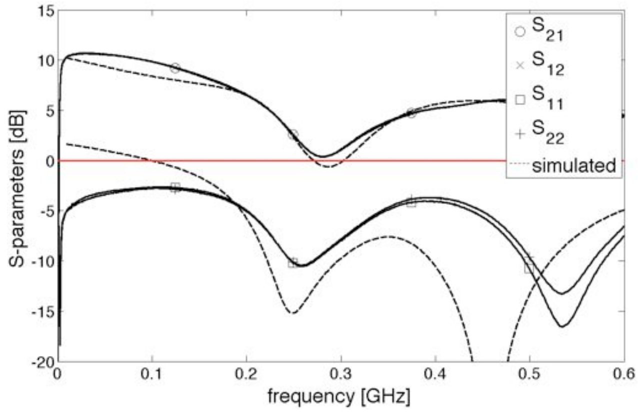

a)

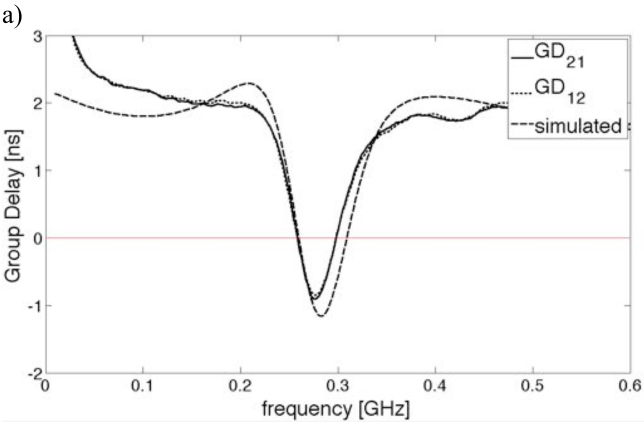

b)

Figure 6a) Measured (solid lines) and simulated (dashed lines) S-parameters of the entire bidirectional NGD circuit and b) the measured and simulated group delay in both directions.

3. Bidirectional Time-Domain Pulse Propagation

The bidirectional and stable NGD operation of the circuit is demonstrated in the time-domain by propagation of the same Gaussian modulated pulse through the circuit in both directions. The time-domain reflectometry experiment shown in Fig. 7 is employed (using a Rohde & Schwarz SMT03 RF generator, Agilent 33250A signal generator and Agilent DSO7104A oscilloscope). The setup uses 50Ω delay lines, with delays TD_1 and TD_2, to separate the incident, reflected and two-way transmitted pulses for a device under test (DUT) inserted in the propagation path. A short-circuit load is placed at the end of the second delay line so that the same pulse transmitted in the forward direction through the DUT is reflected back and is transmitted through it in the reverse direction. Fig. 7b shows an example of the measured waveform when the bidirectional NGD circuit is the DUT. It clearly indicates the incident pulse, the reflected pulse from the input to the DUT (due to non-zero S_{11}) and the two-way transmitted pulse (transmitted through the DUT, reflected back from the load, and transmitted back through the DUT in the opposite direction). Three different devices were used for the DUT; a very short 15 ps delay line, a 443 ps delay line (approximately equal to the speed-of-light delay across the

14.5 cm physical length of the NGD circuit), and the bidirectional NGD circuit.

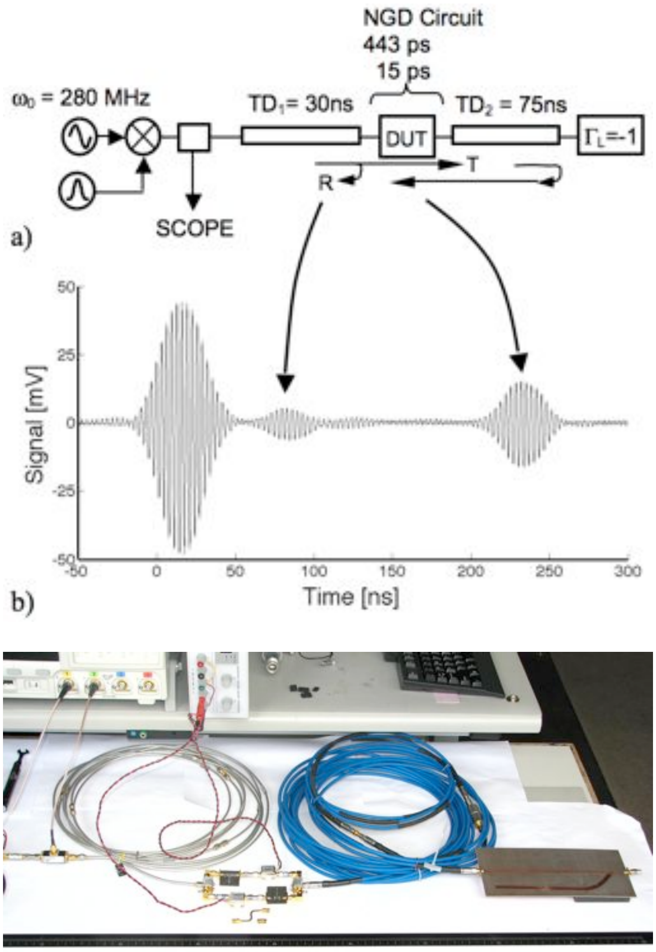

c)

Figure 7a) Time-domain reflectometry measurement of a 14MHz bandwidth Gaussian pulse modulated at 280MHz as it propagates in both directions through the DUT, b) example sampled waveform indicating incident, reflected and two-way transmitted pulses, and c) photograph of the experiment indicating (from left to right), 10x coupler for signal sampling, coiled 30ns delay line, the NGD circuit, coiled 75ns delay line and reflective load.

The measured two-way transmitted pulses for the three devices are shown in Fig. 8a. Fig. 8b shows the normalized envelopes of the three two-way transmitted pulses. A three-parameter fit of the Gaussian envelopes was used to determine the delays of the pulse peaks of the 443 ps delay line and the NGD circuit, relative to the 15 ps delay line peak. The measured two-way delay of the pulse peak for the 443 ps delay line was 965 ps (one-way delay GD_{21} = 482 ps). The measured delay for the NGD circuit was -1.200 ns (one-way delay GD_{21} = -600 ps). The amplitude of the peak of the NGD device waveform is slightly amplified, by a factor of 1.25 (1.12 for one-way transmission), with respect to the other two devices due to the slightly greater-than-unity overall gain for a finite bandwidth signal ($|S_{21}(\omega)|$ is slightly larger than unity at frequencies other than the resonant frequency). The pulse shape for the NGD device is also slightly distorted, as expected, due to the dispersive frequency response near the resonant frequency. The frequency and two-way time-domain experiments clearly demonstrate the ability to advance a finite bandwidth pulse through a medium in both directions without attenuation.

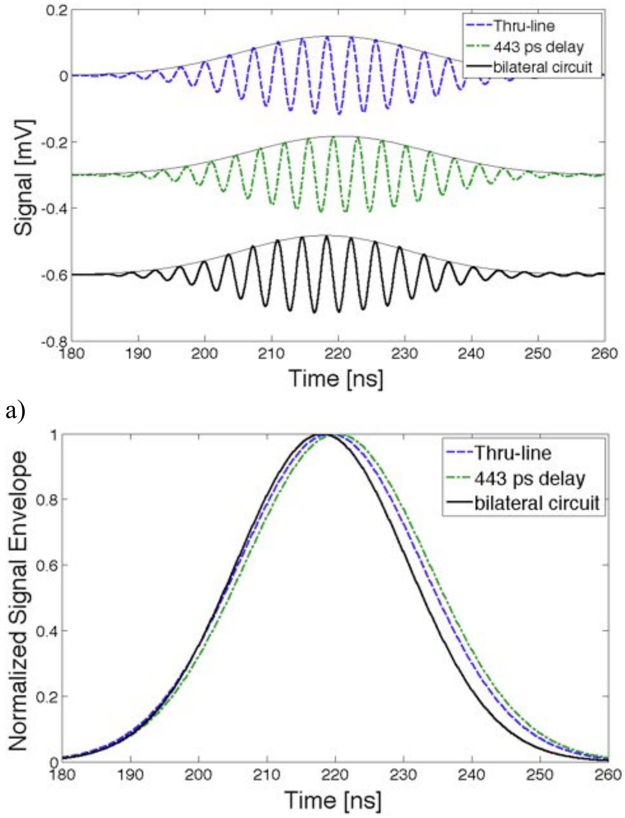

b)

Figure 8a) Measured two-way transmitted 280 MHz modulated pulses through; a 15 ps thru-line, a 443 ps delay line, and the bidirectional NGD circuit and b) the envelopes of the pulses, indicating two-way peak delays of 965 ps for the 443 ps delay line and -1.200 ns for the NGD circuit relative to the 15 ps delay line.

4. Bidirectional Circuit Stability

Due to the large out-of-band gain, $|S_{21}(\omega\to 0)|\sim A_{tot}>1$, and the greater-than-unity reverse transmission coefficient, $|S_{12}(\omega)|=|S_{21}(\omega)|>1$, the bidirectional circuit is potentially unstable. For the demonstrated NDG circuit, the measured input and output reflection coefficients are less than 0 dB for all frequencies as shown in Fig. 6a, making the bilateral circuit stable for the case of matched terminations ($|\Gamma_{IN}|=|S_{11}(\omega)|=|\Gamma_{OUT}|=|S_{22}(\omega)|<1$ for $|\Gamma_L|,|\Gamma_S|=0$, where Γ_L is the load termination reflection coefficient and Γ_S is the source termination reflection coefficient). To analyze the stability of the bidirectional circuit, the input and output reflection coefficients for the general termination case are considered. For stable operation [18], the following conditions must be met,

$$|\Gamma_{IN}| = \left| S_{11} + \frac{S_{21}^2 \Gamma_L}{1 - \Gamma_L S_{22}} \right| < 1 \,, |\Gamma_{OUT}| = \left| S_{22} + \frac{S_{12}^2 \Gamma_S}{1 - \Gamma_S S_{11}} \right| < 1 \cdot \qquad (13)$$

Using (13), and the S-parameters of the bidirectional circuit, the range of load and source impedance values for which the circuit will be stable can be identified. Using expressions for identifying the regions of instability [18] a conditional stability analysis was performed to identify the range of impedances for which the circuit remains stable. The analysis was performed using the NGD design equations (3-4), (7-12), with a resonant frequency of f_0=280 MHz, a Q = 2.62 and an out-of-band gain A_{tot} = 2.84 (9.1 dB). Since the power combiners have a finite isolation and an insertion loss, these will affect the stability results. For L=$1/2^{1/2}$ (3dB insertion loss) and varying values of isolation, I, Fig. 9 indicates the maximum magnitude of the complex termination reflection coefficient, $|\Gamma|_{max}$, for which the circuit is stable ($|\Gamma_L|_{max}$ = $|\Gamma_S|_{max}$ due to the symmetry of S). This is a lower limit since the circuit could possibly be stable for larger magnitudes but only for certain angles. Fig. 9 indicates that, for stable operation under different load conditions, the combiner isolation should be as large as possible. At frequencies near f_0, the circuit is stable for almost all values of $|\Gamma|$. The dashed line in Fig. 9 gives $|\Gamma|_{max}$ for the designed NGD bidirectional circuit using the actual measured combiner values, L = 0.69 (insertion loss = 3.2dB) and I = 0.045 (isolation = 27dB).

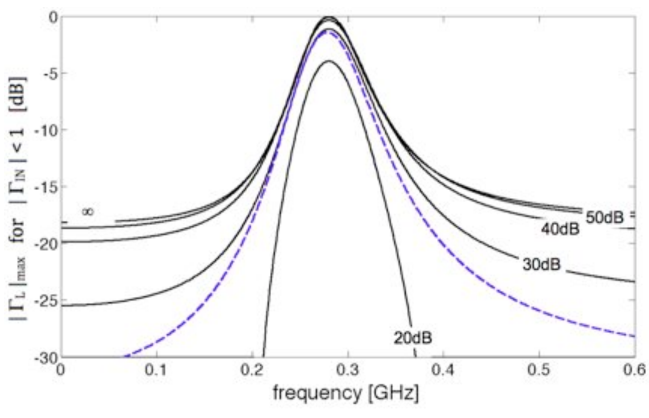

Figure 9: Maximum termination reflection coefficient magnitude, $|\Gamma_L|_{max}$, for stable operation using combiners with insertion loss of 3dB and various isolation, I, values for the NGD design: f_0=280 MHz, Q = 2.62, A_{tot} = 2.84. The dashed curve is for the combiner used in this study with an insertion loss of 3.2dB and isolation of 27dB.

5. Conclusions

A bidirectional, conditionally stable gain-compensated circuit exhibiting lossless NGD was presented. The frequency and two-way time-domain experiments clearly demonstrate the ability to advance a finite bandwidth pulse through a medium in both directions without attenuation. The design operates at 280 MHz, but it can be extended to higher frequency through design of the NGD resonator and proper choice of amplifiers and power splitters. The amplifier used in this work has a wide bandwidth (4 GHz) with a flat group delay response and thus can be used well into the GHz region. The combiner isolation is critical for stable circuit operation and should be chosen such that $|S_{21}^{AB}I|$<<1 and $|S_{11}^{AB}I|$<<1. This implies that $|GI|$<<1 and, since G is related to the desired NGD-bandwidth through A_{tot} (GL^2/A_{tot} =1), this places a limit on the minimum required isolation characteristic of the combiner.

The bidirectional NGD device has several applications in minimization of transmitting/receiving beam-squint in linear phased arrays, bidirectional baluns, or bidirectional 90° feed for circular polarization of antennas. The circuit could also be used to compensate for propagation delays in interconnect circuits. It should be pointed out though that information transmission through the circuit will always be luminal and any discontinuity in a signal waveform, or its derivatives, will propagate at a velocity not exceeding that of the speed of light in a vacuum. In the time-domain, NGD circuits cause the output peak of a well-behaved wave packet or a smooth pulse to precede the input peak. This is achieved through pulse reshaping (rephrasing) as a result of the anomalous dispersive behavior of the circuit and does not violate causality. Lastly, by matching the NGD to the speed-of-light delay across the physical length, l, of the circuit ($GD_{21} = l/c$), would make possible construction of a finite size medium exhibiting the properties of a one-dimensional spatial void for finite bandwidth smooth waveform signals.

Acknowledgements

This work was supported by the Natural Sciences and Engineering Research Council of Canada. Use of the facilities of the Advanced RF Systems Lab of the National Microelectronics and Photonics Testing Collaboratory are appreciated.

References

[1] A. Dogariu, A. Kuzmich and L.J. Wang, Transparent anomalous dispersion and superluminal light-pulse propagation at negative group velocity, *Physical Rev. A*, 63-053806, 2001.

[2] O.F. Siddiqui, M. Mojahedi and G.V. Eleftheriades, Periodically loaded transmission line with effective negative refractive index and negative group velocity, *IEEE Trans. Antennas Propag.* 51: 2619–2625, 2003.

[3] B. Ravelo, A. Perannec, M. LeRoy and Y.G. Boucher, Active microwave circuit with negative group delay, *IEEE Microwave Wireless Comp. Lett.* 17: 861-863, 2007.

[4] S. Gharavi and M. Mojahedi, Theory and application of gain-assisted periodically loaded transmission lines with negative or superluminal group delays, *Proc. IEEE Intl. Conf. Antennas Propag.*, Aloha, Hawaii, pp. 2373-2376, June 2007.

[5] T. Nakanishi, K. Sugiyama and M. Kitano, Demonstration of negative group delays in a simple electronic circuit, American J. Physics, 70: pp. 1117-1121, Nov. 2002.

[6] B. Ravelo, A. Perennec and M. Le Roy, Negative group delay active topologies respectively dedicated to microwave frequencies and baseband signals, *J. EuMA*, 4: pp. 124-130, Jun. 2008.

[7] M. Kandic and G.E. Bridges, Asymptotic limits of negative group delay in active resonator-based distributed devices, *IEEE Trans. Circuits and Systems-I*, 58: 1727-1735, 2011.

[8] B. Ravelo, A. Perennec, M. Le Roy and Y. Boucher, Synthesis of broadband balun negative group delay active circuits, *Proc. IEEE Intl. Conf. Antennas Propag.*, Aloha, Hawaii, June 2007.

[9] B. Ravelo, A. Perennec and M. Le Roy, Broadband balun using active negative group delay circuit, *Proc.* 2007 *European Microwave Conference*, pp. 466–469, Oct. 2007.

[10] S. Hrabar, I. Krois and A. Kiricenko, Towards active dispersionless ENZ metamaterial for cloaking applications, *Metamaterials* 4: 89-97, 2010.

[11] M. Kandic and G.E. Bridges, Bilateral gain-compensated negative group delay circuit, *IEEE Microwave Wireless Comp. Lett.* 21: 308-310, 2011.

[12] H. Noto, K. Yamauchi, M. Nakayama and Y. Isota, Negative group delay circuit for feed-forward amplifier, *Proc., 2007. IEEE/MTT-S Intl. Microwave Symp.*, pp. 1103–1106, June 2007.

[13] S. Keser and M. Mojahedi, Broadband negative group delay microstrip phase shifter design, *Proc. IEEE Intl. Conf. Antennas Propag.*, Charleston, South Carolina, June 2009.

[14] B. Ravelo, M. Le Roy and A. Perennec, Application of negative group delay active circuits to the design of broadband and constant phase shifters, *Microwave And Optical Technology Letters*: 50: pp. 3078-3080, Dec. 2008.

[15] S.S. Oh and L. Shafai, Compensated circuit with characteristics of lossless double negative materials and its application to array antennas," *IET Microwaves, Antennas Propag.*, 1: pp. 29-38, Jan. 2007.

[16] O.F. Siddiqui, S.J. Erickson, G.V. Eleftheriades and M. Mojahedi, Time-domain measurement of negative group delay in negative-refractive-index transmission-line metamaterials, *IEEE Trans. Microwave Theory Tech.* 52: 1449-1454, 2004.

[17] S.J. Erickson, M. Khaja and M. Mojahedi, Time-and frequency-domain measurements for an active negative group delay circuit, *Proc. IEEE Intl. Conf. Antennas Propag.*, pp. 790-793, July 2005.

[18] D.M. Pozar, *Microwave Engineering*. John Wiley & Sons, New York, 2nd edition, chapter 11, pp. 612-618, 1998.